Seasonal regulation of the lncRNA *LDAIR* modulates self-protective behaviors during the breeding season

Tomoya Nakayama[1, 5*], Tsuyoshi Shimmura[1, 5, 8*]†, Ai Shinomiya[1, 8], Kousuke Okimura[5, 7], Yusuke Takehana[2, 8]††, Yuko Furukawa[7], Takayuki Shimo[1, 5], Takumi Senga[1, 5], Mana Nakatsukasa[1, 5], Toshiya Nishimura[3]‡, Minoru Tanaka[3, 8]‡, Kataaki Okubo[9], Yasuhiro Kamei[4, 8], Kiyoshi Naruse[2, 8], Takashi Yoshimura[1, 5 -7**]

[1]Division of Seasonal Biology, [2]Laboratory of Bioresources, [3]Laboratory of Molecular Genetics for Reproduction, [4]Spectrography and Bioimaging Facility, National Institute for Basic Biology, Okazaki, Aichi 444-8585, Japan; [5]Laboratory of Animal Integrative Physiology, [6]Avian Bioscience Research Center, Graduate School of Bioagricultural Sciences, [7]Institute of Transformative Bio-molecules (WPI-ITbM), Nagoya University, Nagoya, Aichi 464-8601, Japan; [8]Department of Basic Biology, The Graduate University for Advanced Studies (SOKENDAI), Miura, Kanagawa 240-0193, Japan; [9]Department of Aquatic Bioscience, Graduate School of Agricultural and Life Sciences, The University of Tokyo, Bunkyo, Tokyo 113-8657, Japan

[**]Correspondence:
Takashi Yoshimura, Ph.D., FRSB
Professor of Integrative Physiology
Institute of Transformative Bio-Molecules (WPI-ITbM)
Nagoya University
Furo-cho, Chikusa-ku, Nagoya 464-8601, Japan
E-mail: takashiy@agr.nagoya-u.ac.jp

Present address: †Department of Biological Production, Tokyo University of Agriculture and Technology, Fuchu, Tokyo 183-8509, Japan; ††Department of Bio-Science, Nagahama Institute of Bio-Science and Technology, Nagahama, Shiga 526-0829, Japan; ‡Division of Biological Science, Graduate School of Science, Nagoya University, Nagoya, Aichi 464-8601, Japan

[*]These authors contributed equally to this work.

Abstract

To cope with seasonal environmental changes, animals adapt their physiology and behavior in response to photoperiod. However, the molecular mechanisms underlying these adaptive changes are not completely understood. Here we show using genome-wide expression analysis that an uncharacterized long non-coding RNA (lncRNA), *LDAIR*, is strongly regulated by photoperiod in medaka fish (*Oryzias latipes*). Numerous transcripts and signaling pathways are activated during the transition from short day (SD) to long day (LD) conditions, but *LDAIR* is one of the first genes to be induced, and its expression shows a robust daily rhythm in LD. Transcriptome analysis of *LDAIR* knockout (KO) fish reveals that the *LDAIR* locus regulates a gene neighborhood, including *corticotropin releasing hormone receptor 2* (*CRHR2*), which is involved in the stress response. Behavioral analysis of *LDAIR* KO fish demonstrates that *LDAIR* affects self-protective behaviors under LD conditions. We therefore propose that photoperiodic regulation of *CRHR2* by *LDAIR* modulates adaptive behaviors to seasonal environmental changes.

During the breeding season, animals show stress responses, such as self-protective and escape behaviors[1], when confronted with potentially dangerous situations (e.g., predation, interspecific competition, and harsh weather). These behaviors are critical for animals to survive the changing environment. Photoperiod is the most reliable indicator of the forthcoming season, and seasonal regulation of various physiological and behavioral processes by photoperiod (so-called photoperiodism) has been known for decades[2, 3]. However, the molecular mechanisms underlying seasonal adaptive strategies are not well understood. Japanese medaka fish (*Oryzias latipes*) serve as an excellent model to study the mechanism of seasonal adaptation, because of their highly sophisticated seasonal responses and the recent availability of genomic information and genome-editing tools[4-9]. Interestingly, we recently demonstrated that dynamic seasonal changes in color perception alters breeding behavior in medaka[8]. To further understand the molecular basis of seasonal adaptation in medaka, we performed genome-wide transcriptome analysis during the transition from short day (SD) to long day (LD) conditions and identified several photoperiodically-regulated genes and signaling pathways. Among these, we focused on a novel, long non-coding RNA (lncRNA, *LDAIR*), whose robust rhythmic expression was induced only under LD conditions. Transcriptome analysis of *LDAIR* knockout (KO) fish reveals differential expression of a number of genes close to the *LDAIR* locus, including *corticotropin releasing hormone receptor 2* (*CRHR2*), which is known to be involved in the stress response[10, 11]. Behavioral

analysis of *LDAIR* KO medaka suggests that *LDAIR* affects stress-associated protective behaviors. These results indicate that photoperiodic regulation of *CRHR2* by the *LDAIR* locus may modulate risk-sensitivity and increase animal fitness to changing environments.

Results

Identification of photoperiodically-regulated transcripts and signaling pathways.

To characterize the transcriptional landscape during the transition from SD to LD, we performed genome-wide expression analysis using customized medaka DNA microarrays (Agilent Technologies). We transferred female medaka kept under SD (10 h light / 14 h dark; 26°C) to LD (16 h light / 8 h dark; 26°C) conditions. The brain region containing the hypothalamus and pituitary were collected from six fish every 4 h for three days during this transition (Supplementary Fig. 1a). For each time point, biotinylated antisense RNAs (cRNAs) prepared from pooled brain samples from three animals were hybridized to duplicate sets of arrays to minimize experimental error (n = 2). One-way ANOVA analysis ($P < 0.01$, Tukey HSD (Honest Significant Difference) post-hoc test, and Benjamini Hochberg FDR (False Discovery Rate), $P < 0.01$) with a 2-fold cut-off and hierarchical cluster analysis were performed. This analysis identified 1,249 transcripts that were differentially expressed (Fig. 1a, Supplementary Data 1). Among these, expression of 143 transcripts were reduced (designated as down-regulated genes) and 758 were increased (designated as up-regulated genes) during the transition to LD (Fig. 1b). To identify photoperiodically-regulated signal transduction pathways, we also performed Ingenuity Pathway Analysis (IPA) based on the microarray data. This canonical pathway analysis detected up-regulation of FXR/RXR and LXR/RXR nuclear receptor signaling, ubiquinol-10 and cholesterol biosynthesis, and down-regulation of acute phase response signaling by LD (Fig. 1c).

In addition to seasonally regulated genes, we detected 348 transcripts that showed a daily rhythm, including the circadian clock genes *ARNTL1A, NPAS2-4, PER1-3*, *CRY1, NR1D2, RORB/C,* and *DEC1* (referred to as cycling genes) (Fig. 1b). Furthermore, we noticed that expression of one transcript named *olvl28m13* (National Bio-Resource Project Medaka database, accession number DK236042) was induced and strongly rhythmic only under LD conditions (red bold line in Fig. 1b). Notably, the timing of its induction was much earlier than nearly all up-regulated genes.

Photoperiodically-regulated, cycling transcript *olvl28m13* is a lncRNA.

According to the National Center for Biotechnology Information (NCBI) database, *olvl28m13* is an uncharacterized lncRNA (GeneID: 105356286). To examine *olvl28m13*

further, we next performed strand-specific RNA-seq analysis and confirmed higher expression under LD than SD conditions (Fig. 2a). This RNA was transcribed from the intronic region of the *LIPIN2* (*LPIN2*) gene (between exon 1 and 2) located on medaka chromosome 17 in the opposite direction of *LPIN2*. Although intronic lncRNAs are often reported to regulate overlapping protein coding genes[12, 13], *olvl28m13* did not overlap with the *LPIN2* transcript, and there was no significant difference in *LPIN2* expression in SD compared to LD (Fig. 2a). To determine the protein-coding potential of this transcript, we next performed ribosomal profiling analysis (Ribo-seq)[14]. RNAs that are translated into protein are associated with ribosomes, whereas those that function as RNAs, such as some lncRNAs, are not. Ribo-seq involves the isolation and sequencing of ribosome-associated RNAs, which then determines the protein coding potential of RNAs. To compare RNA-seq and Ribo-seq directly, we prepared libraries from the same samples. When we analyzed the positive control *beta-actin*, reads from RNA-seq were mapped to the open reading frame (ORF) and untranslated region (UTR), while those from Ribo-seq were mapped only to the ORF, as expected (Fig. 2b). We then examined reads from the negative control, *CYRANO*, one of the few conserved lncRNAs among vertebrates[15]. Almost no reads were mapped from Ribo-seq (Fig. 2b), while many reads were obtained from RNA-seq. These results clearly demonstrate that we can obtain reads from ribosome-protected RNA fragments using Ribo-seq and therefore distinguish between protein-coding and non-protein coding RNAs. We then examined *olvl28m13*. Similar to *CYRANO*, many reads were obtained using RNA-seq, but no reads were detected by Ribo-seq (Fig. 2b) (note that the results from RNA-seq of *olvl28m13* in Figs. 2a and 2b are not identical; this is because the data in Fig. 2a is from strand-specific RNA-seq, while that in Fig. 2b is the result of RNA-seq from both strands.) Taken together, these findings indicate that the transcript *olvl28m13* is not associated with ribosomes and most likely not translated into protein. We therefore categorize *olvl28m13* as a lncRNA that functions as a RNA. Accordingly, we designate this novel lncRNA *long day induced antisense intronic RNA*, *LDAIR*.

LDAIR locus regulates a gene neighborhood.

Many lncRNAs have been reported to regulate the expression of nearby genes, often referred to as a gene neighborhood[16-18]. To examine this possibility for *LDAIR*, we generated KO medaka using the CRISPR/Cas9 system. The *LDAIR* locus was deleted using two different guide RNAs (Fig. 3a). We crossed an injected G0 founder with a wild type (WT) fish to obtain F1 heterozygotes (+/-) and then crossed F1 heterozygotes to generate F2 KO (-/-) and WT (+/+) siblings (Fig. 3b; Supplementary Fig. 2). Genome-wide expression analysis using

DNA microarrays were performed to compare transcripts in brain samples containing hypothalamus and pituitary (Supplementary Fig. 1a) between WT and KO medaka. Biotinylated cRNAs prepared from pooled samples from three fish (total 9 fish for each genotype) were hybridized to triplicate sets of arrays (n = 3). Moderate *t*-test analysis ($P < 0.05$, Tukey HSD post-hoc test, and Benjamini Hochberg FDR, $P < 0.1$) with a 2-fold cut-off identified 33 probes that represented 26 differentially expressed transcripts (Fig. 3c). Interestingly, 10 of the 26 transcripts were located on the same chromosome as *LDAIR* (Chr 17) (Fig. 3d, Supplementary Data 2). Differential expression of 7 of the 10 transcripts was validated by qPCR assay (Supplementary Fig. 3), and these 7 transcripts were located within a range of 1.8 Mb of *LDAIR* (Fig. 3e), suggesting that the *LDAIR* locus might regulate a gene neighborhood. Among these 7 transcripts, 4 transcripts were up-regulated and 3 transcripts (including *LDAIR*) were down-regulated in KO medaka. When we examined the expression of these neighboring genes, *CRHR2* and *ROCK1* were photoperiodically-regulated ($P < 0.05$, *t*-test; n = 6) (Supplementary Fig. 4). Although *CCDC13* and *ADCYAP1R1* were weakly photoperiodic, statistical differences were not observed in other neighboring genes ($P > 0.05$, *t*-test; n = 6) (Supplementary Fig. 4). We then focused our studies on *CRHR2* (Fig. 3e), because CRHR2 is known to be involved in the stress response in mouse[10, 11], and we wanted to test the hypothesis whether *LDAIR* may regulate stress-related behaviors in medaka fish.

LDAIR KO fish show a decrease in self-protective behaviors.

Hyperactivation of the hypothalamic-pituitary-adrenal (HPA) axis and/or extremely high levels of stress hormones are known to inhibit reproduction. By contrast, moderately elevated levels of stress hormones actually facilitate reproduction, and stress responses are typically increased during the breeding season[1, 19]. The HPA axis can function to mediate diverse responses to various stressors and its behavioral effects include promotion of protective and escape behaviors[20]. Thus, stress responses may also eliminate or reduce the impact of potential stressors and hence promote animal survival[21]. When we measured whole-body cortisol levels, an increase in baseline cortisol levels was observed under LD breeding conditions ($P < 0.05$, *t*-test; n = 4) (Fig. 4a).

The novel tank test presents a motivational conflict between the 'protective' diving behavior and vertical 'exploration' behavior[22] (Fig. 4b). When we performed the novel tank test using fish kept under SD conditions (when *LDAIR* expression is suppressed), there were no significant differences in the behaviors between WT and KO medaka (Fig. 4c top). In contrast, WT medaka showed lower vertical exploration and longer freezing duration than KO medaka under LD conditions (when *LDAIR* is expressed) ($P < 0.01$, *t*-test; n = 16) (Fig.

4c bottom). In general, fish avoid brightly lit areas to avoid detection by other animals[22]. When we performed the light-dark tank test (Fig. 4d), no significant changes were observed between WT and KO medaka under SD conditions (Fig. 4e top), as in the case of the novel tank test. Interestingly, however, WT medaka showed more light avoidance behavior than KO medaka under LD conditions ($P < 0.05$, *t*-test; n = 20) (Fig. 4e bottom). These results suggest that WT medaka are more sensitive and avoid potentially dangerous situations more than *LDAIR* KO medaka under LD conditions.

We also examined the effects of *LDAIR* KO on seasonal reproduction, and *LDAIR* KO medaka were fertile, similar to WT, and no significant differences were observed for the photoperiodic regulation of the gonads (Supplementary Fig. 5).

Discussion

In non-tropical areas, organisms are exposed to seasonal changes in the environment. To cope with these changes, animals often adapt their behavior. Although Aristotle described seasonal changes in animal behavior in his 'Historia Animalium,' its underlying mechanisms remain unclear. To better understand this mechanism, we performed transcriptome analysis and identified multiple signal transduction pathways that are regulated by changing photoperiod. For example, pathways related to cholesterol metabolism, such as nuclear receptors FXR/RXR and LXR/RXR and cholesterol biosynthesis, were activated by LD. Cholesterol within the brain is an essential component of synapses and required for dendrite formation[23, 24] and axonal guidance[25]. Therefore, it seems possible that activation of pathways related to cholesterol metabolism may modulate neuronal plasticity to prepare for the coming spring.

In addition to these signaling pathways, we discovered photoperiodic regulation of the lncRNA *LDAIR*. Interestingly, induction of *LDAIR* was time-of-day dependent (Fig. 1). We therefore searched for circadian clock-controlled DNA sequences (E/E'-box [CACGT(T/G)], D-box (DBP response element) [TTATG(C/T)AA], and RRE (RevErbA response element) [(A/T)A(A/T)NT(A/G)GGTCA]) within intron 1 of *LPIN2,* where *LDAIR* is localized. We found one D-box 81 bp upstream of the *LDAIR* transcription start site (Fig. 2b). Notably, D-boxes have been demonstrated to be important DNA elements regulating light-inducible genes in zebrafish[27]. However, enhancers may also be located far from transcription start sites of genes (e.g., ~1 Mb upstream or downstream). Thus, the regulatory mechanism of *LDAIR* expression remains to be determined. Transcriptome and behavioral analyses of *LDAIR* KO medaka demonstrated differences in the expression of the nearby gene *CRHR2* and in the stress response. Two CRH receptor sub-types, CRHR1 and CRHR2, are conserved in a number of vertebrate species[28]. Even though both receptors are involved in

stress responses, they have opposite functions; *CRHR1* increases anxiety[29, 30], whereas *CRHR2* has a calming, anxiolytic role[10, 11]. In the present study, *LDAIR* KO medaka showed higher *CRHR2* expression and lower sensitivity to stressors (e.g., novel tank and light area). These behavioral phenotypes of *LDAIR* KO fish are consistent with previous reports describing an anxiolytic role for CRHR2. An increase in stress responses during the breeding season has been reported in a number of animals[1]. For example, activation of the HPA axis during the breeding season suppresses territorial behaviors and promotes escape behaviors in white crowned sparrow[20]. We speculate that self-protective behaviors observed in medaka under LD conditions increases risk-sensitivity and hence, fitness during the breeding season.

Recently, lncRNAs have been recognized as important regulators of gene expression[31-34], and some lncRNAs are reported to regulate the expression of nearby genes[16-18]. In the present study, we discovered that the *LDAIR* locus regulates a gene neighborhood. lncRNAs are known to interact with DNA, other ncRNAs, and proteins, and they are implicated in a wide range of transcriptional, posttranscriptional, and posttranslational modifications. They function as guides and decoys, as well as in scaffolding, splicing, mRNA decay and subcellular localization. lncRNAs may influence chromatin architecture by interacting with chromatin-modulating proteins (promoting or preventing recruitment and/or association with chromatin), thereby controlling transcriptional activity; lncRNAs activate or repress transcription by acting locally (near the sites of their transcription: *cis*-regulation) or distally (at sites that are located on other chromosomes: *trans*-regulation) through their ability to recruit regulatory factors to the locus and/or modulate their function; lncRNAs interact with mRNA to regulate splicing, degradation, and translational efficiency; lncRNAs are involved in gene regulation using DNA elements within the lncRNA locus separate from the encoded RNA[33, 34]. To further understand how the *LDAIR* locus influences expression of nearby genes, we attempted to knock down the *LDAIR* transcript in a dose-dependent manner using morpholino oligonucleotides delivered by microinjection into the third ventricle. Unfortunately, knockdown of *LDAIR* was insufficient (~25% reduction) (data not shown), and we could not obtain a clear result. The mechanism of how these neighboring genes are regulated by *LDAIR* should be addressed in future studies.

To our knowledge, this is the first study to report photoperiodically-driven expression of a lncRNA in vertebrates. In general, lncRNAs are not well-conserved across species. However, our homology search analysis suggests that *LDAIR* is conserved at least among various medaka populations (e.g., *Oryzias latipes*, *Oryzias curvinotus*, *Oryzias luzonensis*). Interestingly, several photoperiodically-regulated lncRNAs have recently been reported in plants to regulate photomorphogenesis, cotyledon greening, and

photoperiod-regulated flowering[35-39]. Even though the sequences of lncRNAs are not well-conserved, lncRNAs appear to play an important role across species in the adaptation mechanism to seasonal changes in the environment.

Methods

Animals.

Medaka fish (*Oryzias latipes*) were obtained from a local dealer (Fuji 3A Project, Nagoya, Japan). Medaka were kept under SD (short day; 10 h light / 14 h dark; 26°C) conditions or LD (long day; 16 h light / 8 h dark; 26°C) conditions in a housing system (MEITO system, Meito Suien; LP-30LED-8CTAR, NK system). Light was provided by a white fluorescent light (~7,000 lux) (Supplementary Fig. 6). We used only female fish in our experiments. The timing of sample collection is shown in Supplementary Fig. 1. Animals were treated in accordance with the guidelines of Nagoya University and the National Institutes of Natural Sciences. All experimental protocols were approved by the Animal Experiment Committee of Nagoya University and the National Institutes of Natural Sciences.

DNA microarray analysis.

A customized medaka DNA microarray (Custom Gene Expression Microarray 4 × 44 K, Agilent Technologies) containing 31,150 probes was used for this experiment. In the SD to LD transition experiments, brains were collected from six fish every 4h for three days. In the experiments using *LDAIR*-null fish, brains were collected from nine WT and nine KO fish. Brains were immediately immersed in RNA*later* RNA Stabilization Reagent (QIAGEN) for 1 day, and the brain region containing hypothalamus and pituitary (Supplementary Fig. 1a) was dissected. Total RNA was prepared using an RNeasy Tissue Kit (QIAGEN) and treated with DNase I (QIAGEN) to remove contaminating DNA. cDNA synthesis and cRNA labeling reactions were performed with the Low Input Quick Amp Labeling Kit (Agilent Technologies). Labeled cRNA was purified with RNeasy mini spin columns (QIAGEN) and hybridized using the Gene Expression Hybridization Kit (Agilent Technologies). After washing with Gene Expression Wash Buffer (Agilent Technologies), the glass slide was scanned on a Microarray Scanner (Agilent Technologies).

Ingenuity pathway analysis.

Ingenuity Pathway Analysis (IPA) (https://www.qiagenbioinformatics.com/products/ingenuity-pathway-analysis/) was used to determine which biological processes, pathways and networks were induced or repressed in

LD. Differentially expressed transcripts (1,249) identified in the DNA microarray analysis were used for this analysis and compared at the noon time point in SD (16 h before the LD transition) and LD (32 h after the LD transition). Networks were algorithmically generated based on their connectivity and ranked by Fisher's exact test enrichment statistics. Benjamini-Hochberg corrected *p*-value calculations were then used to identify significantly changed pathways.

Strand specific RNA-seq.

Medaka kept under SD conditions were either maintained in SD or transferred into LD conditions. 16 hours after the transition, brains were collected from six fish for each condition. Brains were immediately immersed in RNA*later* RNA Stabilization Reagent (QIAGEN) for 1 day, and the brain region containing hypothalamus and pituitary (Supplementary Fig. 1a) was then dissected and pooled (n = 3). Total RNA was prepared using an RNeasy Tissue Kit (QIAGEN) and treated with DNase I (QIAGEN) to remove contaminating DNA. Paired-end libraries were constructed from RNA samples using the TruSeq Stranded mRNA LT Sample Prep kit (Illumina) according to the manufacturer's protocol and then sequenced at a read depth of 60 million at 101 bp paired reads using the Illumina HiSeq 4,000 system at Macrogen, Japan. Read quality control was checked using FastQC (http://www.bioinformatics.babraham.ac.uk/projects/fastqc/), and sequences were filtered and trimmed with Trimmomatic[40]. Reads were subsequently mapped to the medaka genome using HISAT2[41].

Ribosome profiling.

To isolate and obtain ribosome-protected fragments (RPFs) from tissue, we modified the first homogenization step of Janich et al., 2015[42]. Medaka kept under SD conditions were transferred into LD conditions and were sacrificed at approximately 16 h after lights on. After isolating whole brain, the brain region containing hypothalamus and pituitary (Supplementary Fig. 1a) was immediately dissected on ice. Each sample was homogenized in 300 µl of lysis buffer (150 mM NaCl, 20 mM Tris-HCI pH 7.4, 5 mM $MgCl_2$, 5 mM DTT, 100 µg/ ml cycloheximide, 1% Triton X-100, 0.5% sodium deoxycholate, complete EDTA-free protease inhibitors (Roche) and 40 U/ ml RNasin plus (Promega)), and incubated on ice for 10 min. The mix was clarified for 3 min at 1,000 g at 4°C, and supernatants were collected, flash-frozen and stored in liquid nitrogen. Lysed supernatants were divided in two for preparation of the RPF libraries and the total RNA libraries. 200 µl of lysed supernatants were incubated with 650 U RNase I (Ambion) and 5 U Turbo DNase (Ambion) for 45 min at

room temperature with gentle mixing. Nuclease digestion was stopped with 8.7 µl of Superase In (Ambion). Lysates were purified on sephacryl S-400 HR spin columns (GE Healthcare Life Sciences). The flow-through was immediately mixed with 1 ml QIAzol Lysis Reagent (QIAGEN) and purified again using the miRNeasy Mini Kit (QIAGEN). The remaining lysed supernatants were also purified using the miRNeasy Mini Kit (QIAGEN) without RNase treatment for the total RNA libraries. Both samples of ribosomal RNA were subtracted using the Ribo-Zero Magnetic Kit (Human/Mouse/Rat) (Illumina), according to the manufacturer's instructions, omitting the 50°C incubation step. RPFs were separated in a 15% urea-polyacrylamide gel, and the region from 28-30 nucleotides was excised and purified by ethanol precipitation. RPF libraries and total RNA libraries were prepared from above RNAs using the TruSeq Ribo Profile Mammalian Library Prep Kit (Illumina) following the manufacturer's protocols. Libraries were sequenced at a read depth of 80 million at 101 bp reads using Illumina HiSeq 2,500 system at Hokkaido System Science Co., Ltd. Read quality control was checked using FastQC (http://www.bioinformatics.babraham.ac.uk/projects/fastqc/), and sequences were filtered and trimmed with a FASTX-Toolkit (http://hannonlab.cshl.edu/fastx_toolkit/index.html). Reads were subsequently mapped to the medaka genome using TopHat[43].

Genome editing using the CRISPR/Cas9 system.

The single guide RNA (sgRNA) expression vector (pDR274; Addgene plasmid 42,250) was linearized with BsaI and purified using NucleoSpin Gel and PCR Clean-up (Takara Bio). Appropriately designed oligonucleotides were synthesized with oligonucleotide purification cartridge (OPC) purification at Eurofins Genomics. A pair of complementary oligonucleotides were annealed by heating at 95°C for 2 min and then cooling slowly to 25°C in 30 min. Annealed oligonucleotides were ligated into the linearized pDR274 vector. Following linearization of the oligonucleotide-inserted pDR274 vector and the Cas9 expression vector (hCas9; gifted by Prof. Zhang of Massachusetts Institute of Technology) with DraI and NotI respectively, the sgRNAs and the capped Cas9 mRNA were synthesized by using the AmpliScribe T7-Flash Transcription Kit (Epicentre) and the mMESSAGE mMACHINE SP6 Transcription Kit (Thermo Fisher Scientific) respectively. Both RNAs were purified using the RNeasy Mini Kit (QIAGEN). A mixed solution of the sgRNAs (50 ng/ µl) and the Cas9 mRNA (100 ng/ µl) were microinjected into one-cell stage embryos using a fine glass needle. *LDAIR* knockout medaka were genotyped using PCR primers 5'-GTGAAATGAAGTGTCCCCAGC-3' and 5'-TGTCTGGGCTTATTGAAACCT-3', and amplicons were analyzed on a microchip electrophoresis system (MCE-202 MultiNA;

Shimazu). Mutant alleles were identified by direct sequencing of the PCR product.

Quantitative PCR.

Reverse transcription was performed on total RNA (200 ng) using the ReverTra Ace qPCR RT Kit (Toyobo). Samples contained SYBR Premix Ex Taq II (Takara), 0.4 μM gene-specific primers (Supplementary Table 1), and 2 μL synthesized cDNA in a 20 μL volume. qPCR was performed on an Applied Biosystems QuantStudio 3 Real-Time PCR System as follows: 95°C for 30 s, followed by 40 cycles of 95°C for 5 s, 60°C for 34 s. Housekeeping gene, *RPL7*, was used as an internal control.

Measurement of cortisol by ELISA.

Since cortisol levels change dramatically at light onset and the phase of the circadian clock is affected by photoperiod, samples were collected in the middle of the day for both LD and SD conditions (LD: zeitgeber time (ZT) 8; SD: ZT 5). Lipid extraction was performed following the protocol of Kikuchi et al., 2015[44]. Four fish were used for each condition. Whole bodies were homogenized in phosphate-buffered saline using Multi-beads shocker (Yasui Kikai Corporation). Lipids were extracted with chloroform/methanol (2:1 v/v) and purified on a Sep-Pak C18 cartridge (Waters Corporation). Cortisol levels were measured using the Cortisol ELISA Kit (Cayman Chemical Company) following the manufacturer's protocol.

Behavioral tests.

All behavioral tests were performed just after light onset (ZT 0). For the novel tank test, fish were introduced into a test tank (100 mm width × 65 mm depth × 142 mm height) filled with water to a height of 100 mm. Behavior was recorded for 22 min by video cameras (Panasonic HC-V230M and JVCKENWOOD GZ-F117), with the first and last minutes of recording excluded from the analysis. Vertical activity and freezing duration were measured using the behavioral analysis software UMATracker (http://ymnk13.github.io/UMATracker/).

For the light-dark tank test, a plastic container was used (150 mm width × 100 mm depth × 55 mm height) and divided into two sections of equal size by covering the bottom and side areas with white- or black-colored opaque tape. Fish were placed in the light area and allowed to move freely between the dark and light areas for 20 min. Time spent in the light area and the total number of transitions from one area to the other area were measured.

Statistical analysis.

Data are presented as the mean + SEM. *F*-tests were used to determine variance. The data

with a normal distribution were analyzed by a Student's *t*-test between two groups. Where variance was significantly different between groups, a Welch's *t*-test was used. Microarray data were analyzed using the GeneSpring software (Agilent Technologies).

Data availability.

The microarray and RNA-seq data are available at NCBI Gene Expression Omnibus (accession number GSE119905). All other data are available from the authors upon request.

References

1. Romero, L. M. Seasonal changes in plasma glucocorticoid concentrations in free-living vertebrates. *Gen. Comp. Endocrinol.* **128,** 1−24 (2002).
2. Rowan, W. Relation of light to bird migration and developmental changes. *Nature* **115,** 494−495 (1925).
3. Follett, B. K. & Sharp, P. J. Circadian rhythmicity in photoperiodically induced gonadotrophin release and gonadal growth in the quail. *Nature* **223,** 968−971 (1969).
4. Egami, N. Effect of artificial photoperiodicity on time of oviposition in the fish, *Oryzias latipes*. *Annot. Zool. Japon* **27**, 57−62 (1954).
5. Awaji, M. & Hanyu, I. Temperature-photoperiod conditions necessary to begin the spawning season in wild type medaka. *Nippon Suisan Gakkaishi* **55**, 747 (1989).
6. Kasahara, M. et al. The medaka draft genome and insights into vertebrate genome evolution. *Nature* **447,** 714−719 (2007).
7. Ansai, S. & Kinoshita, M. Targeted mutagenesis using CRISPR/Cas system in medaka. *Biol. Open* **3,** 362−371 (2014).
8. Shimmura, T. et al. Dynamic plasticity in phototransduction regulates seasonal changes in color perception. *Nat. Commun.* **8,** 412 (2017).
9. Ichikawa, K. et al. Centromere evolution and CpG methylation during vertebrate speciation. *Nat. Commun.* **8,** 1833 (2017).
10. Bale, T. L. et al. Mice deficient for corticotropin-releasing hormone receptor-2 display anxiety-like behaviour and are hypersensitive to stress. *Nat. Genet.* **24,** 410−414 (2000).
11. Kishimoto, T. et al. Deletion of *Crhr2* reveals an anxiolytic role for corticotropin-releasing hormone receptor-2. *Nat. Genet.* **24,** 415−419 (2000).
12. Heo, J. B. & Sung, S. Vernalization-mediated epigenetic silencing by a long intronic noncoding RNA. *Science* **331,** 76−79 (2011).
13. Salameh, A. et al. PRUNE2 is a human prostate cancer suppressor regulated by the intronic long noncoding RNA *PCA3*. *Proc. Natl. Acad. Sci.* **112,** 8403−8408 (2015).

14. Ingolia, N. T., Ghaemmaghami, S., Newman, J. R. S. & Weissman, J. S. Genome-wide analysis in vivo of translation with nucleotide resolution using ribosome profiling. *Science* **324,** 218−223 (2009).
15. Hezroni, H. et al. Principles of long noncoding RNA evolution derived from direct comparison of transcriptomes in 17 species. *Cell Rep.* **11,** 1110−1122 (2015).
16. Engreitz, J. M. et al. Local regulation of gene expression by lncRNA promoters, transcription and splicing. *Nature* **539,** 452−455 (2016).
17. Joung, J. et al. Genome-scale activation screen identifies a lncRNA locus regulating a gene neighbourhood. *Nature* **548,** 343−346 (2017).
18. Werner, M. S. et al. Chromatin-enriched lncRNAs can act as cell-type specific activators of proximal gene transcription. *Nat. Struct. Mol. Biol.* **24,** 596−603 (2017).
19. Moore, I. T. & Jessop, T. S. Stress, reproduction, and adrenocortical modulation in amphibians and reptiles. *Horm. Behav.* **43,** 39−47 (2003).
20. Wingfield, J. C. et al. Ecological bases of hormone—behavior interactions: The "Emergency Life History Stage". *Am. Zool.* **38,** 191−206 (1998).
21. Balm, P. H. M. Stress Physiology in Animals. *Sheffield Academic Press*. (1999).
22. Kysil, E. V. et al. Comparative analyses of zebrafish anxiety-like behavior using conflict-based novelty tests. *Zebrafish* **14,** 197−208 (2017).
23. Goritz, C., Mauch, D. H. & Pfrieger, F. W. Multiple mechanisms mediate cholesterol-induced synaptogenesis in a CNS neuron. *Mol. Cell. Neurosci.* **29,** 190−201 (2005).
24. Fester, L. et al. Cholesterol-promoted synaptogenesis requires the conversion of cholesterol to estradiol in the hippocampus. *Hippocampus* **19,** 692−705 (2009).
25. Posse de Chaves, E. I., Rusinol, A. E., Vance, D. E., Campenot, R. B. & Vance, J. E. Role of lipoproteins in the delivery of lipids to axons during axonal regeneration. *J. Biol. Chem.* **272,** 30766−30773 (1997).
26. Minami, Y., Ode, K. L. & Ueda, H. R. Mammalian circadian clock: the roles of transcriptional repression and delay. *Handb. Exp. Pharmacol.* **217,** 359-377 (2013).
27. Mracek, P. et al. Regulation of per and cry genes reveals a central role for the D-box enhancer in light-dependent gene expression. *PLoS ONE* **7**, e51278 (2012).
28. Seasholtz, A. F., Valverde, R. A. & Denver, R. J. Corticotropin-releasing hormone-binding protein: Biochemistry and function from fishes to mammals. *J. Endocrinol.* **175,** 89−97 (2002).
29. Timpl, P. et al. Impaired stress response and reduced anxiety in mice lacking a functional corticotropin-releasing hormone receptor 1. *Nat. Genet.* **19,** 162−166 (1998).

30. Smith, G. W. et al. Corticotropin releasing factor receptor 1-deficient mice display decreased anxiety, impaired stress response, and aberrant neuroendocrine development. *Neuron* **20,** 1093−1102 (1998).
31. Wang, K. C. & Chang, H. Y. Molecular mechanisms of long noncoding RNAs. *Mol. Cell* **43,** 904−914 (2011).
32. Guttman, M. & Rinn, J. L. Modular regulatory principles of large non-coding RNAs. *Nature* **482,** 339−346 (2012).
33. Yang, G., Lu, X. & Yuan, L. LncRNA: A link between RNA and cancer. *Biochim. Biophys. Acta* **1839,** 1097−1109 (2014).
34. Sun, Q., Hao, Q. & Prasanth, K. V. Nuclear long noncoding RNAs: Key regulators of gene expression. *Trends Genet.* **34,** 142−157 (2018).
35. Ding, J. et al. A long noncoding RNA regulates photoperiod-sensitive male sterility, an essential component of hybrid rice. *Proc. Natl. Acad. Sci.* **109,** 2654−2659 (2012).
36. Wang, Y. et al. Arabidopsis noncoding RNA mediates control of photomorphogenesis by red light. *Proc. Natl. Acad. Sci.* **111,** 10359−10364 (2014).
37. Wang, Y., Li, J., Deng, X-W., & Zhu, D. Arabidopsis noncoding RNA modulates seedling greening during deetiolation. *Sci. China Life Sci.* **61**, 199−203 (2018).
38. Henriques, R. et al. The antiphasic regulatory module comprising *CDF5* and its antisense RNA *FLORE* links the circadian clock to photoperiodic flowering. *New Phytol.* **216**, 854−867 (2017).
39. Sánchez-Retuerta, C., Suaréz-López, P. & Henriques, R. Under a new light: Regulation of light-dependent pathways by non-coding RNAs. *Front. Plant Sci.* **9,** 962 (2018).
40. Bolger, A. M. et al. Trimmomatic: a flexible trimmer for illumina sequence data. *Bioinformatics*, **30**, 2114−2120 (2014).
41. Kim, D., Langmead, B. & Salzberg, S. L. HISAT: a fast spliced aligner with low memory requirements. *Nat. Methods* **12**, 357−360 (2015).
42. Janich, P., Arpat, A. B., Castelo-Szekely, V., Lopes, M. & Gatfield, D. Ribosome profiling reveals the rhythmic liver translatome and circadian clock regulation by upstream open reading frames. *Genome Res.* **25,** 1848−1859 (2015).
43. Trapnell, C., Pachter, L. & Salzberg, S. L. TopHat: discovering splice junctions with RNA-Seq. *Bioinformatics* **25**, 1105−1111 (2009).
44. Kikuchi, Y., Hosono, K., Yamashita, J., Kawabata, Y. & Okubo, K. Glucocorticoid receptor exhibits sexually dimorphic expression in the medaka brain. *Gen. Comp. Endocrinol.* **223,** 47−53 (2015).

Acknowledgements

We thank the NBRP-Medaka (National Bio-Resource Project of MEXT, Japan) and the Data Integration and Analysis Facility for use of their facilities. We also thank M. Okubo, A. Akama, N. Baba, and C. Kinoshita for technical assistance, and Dr. T.K. Tamai for comments on the manuscript. This work was supported in part by the JSPS KAKENHI "Grant-in-Aid for Specially Promoted Research" (26000013), the Human Frontier Science Program (RGP0030/2015), and Grant-in-Aid for JSPS Fellows (18J10936). WPI-ITbM is supported by the World Premier International Research Center Initiative (WPI), MEXT, Japan.

Author contributions

T.Y. conceived the research. T.Na., T. Shimmura and T.Y. designed the research. T. Shimmura, T. Shimo, T. Senga and T.Y. performed the microarray analysis for the SD to LD transition experiments. T.Na., K. Okimura and T.Y. performed Ingenuity pathway analysis. T.Na. and Y.F. performed strand specific RNA-seq. T.Na. performed ribosome profiling, qPCR analysis, cortisol measurement and behavioral assays. T.Na., T. Shimmura, Y.T., T. Shimo, M.N. generated and genotyped *LDAIR* KO medaka. T.Na. and A.S. performed the microarray analysis for the experiment using *LDAIR* KO fish. T.Ni. and M.T. provided Medaka microarrays. Y.K., K.N., and K. Okubo provided new methods and materials. T.Na. and T.Y. wrote the manuscript. All authors discussed the results and commented on the manuscript.

Competing financial interests

The authors declare no competing financial interests.

Figure legends

Fig. 1 Transcriptional landscape during the transition from SD to LD.

a Hierarchical clustering of 1,249 transcripts in a brain region containing hypothalamus and pituitary following transfer into LD conditions. Data were normalized to the entire data set. The color scale represents normalized signal intensity. The colored bar at the right represents the clustered category. **b** Expression pattern of down-regulated (top), cycling (middle), and up-regulated (below) genes in response to LD stimulus. The red bold line in the cycling genes panel represents the expression pattern of *olvl28m13*. **c** Top 5 significantly changed canonical signaling pathways during the transition to LD.

Fig. 2 *olvl28m13* is a long non-coding RNA.

a Strand-specific RNA-seq identified *olvl28m13* in the intronic region of the *LPIN2* gene, which is located on chromosome 17 and transcribed from the opposite strand. The abundance of reads mapping within the *olvl28m13* and *LPIN2* genomic loci is shown. The color corresponds to the DNA strand, with the sense strand in red and antisense strand in blue. The number on the right represents the range of the read density. **b** Protein coding potential revealed by ribosome profiling. Alignment of RNA-seq (black) or Ribo-seq (orange) reads at the *beta-actin*, *CYRANO*, and *olvl28m13* (*LDAIR*) loci. The open black boxes indicate the predicted untranslated regions of *beta-actin*. The number on the right represents the range of the read density. D-box (DBP response element: [TTATGCAA]).

Fig. 3 The *LDAIR* locus regulates a gene neighborhood.

a Genomic region targeted and deleted by CRISPR/Cas9 system guide RNAs. Blue bars represent *LDAIR* exons. Red bars represent *LPIN2* exons. Target sequences of the guide RNAs (gRNA) are shown above the deleted region. **b** PCR fragments obtained from genomic DNA of WT (1,788 bp), heterozygous mutant (1,788 and 318 bp) and KO (318 bp) analyzed by a microchip electrophoresis system. **c** Volcano plot of differentially expressed transcripts between WT and KO medaka detected by microarray. Each point represents the mean expression level plotted against the fold change. Red points are up-regulated transcripts, and blue points are down-regulated transcripts ($P < 0.05$, Tukey HSD post-hoc test, and Benjamini Hochberg FDR, $P < 0.1$ with a 2-fold cut-off for fold change) in KO fish. Gray points show transcripts with no significant change. **d** Number of differentially expressed transcripts on each chromosome. All sections without a number indicate only one differentially expressed gene. **e** Genomic locus of *LDAIR*, and neighboring genes that are

differentially expressed in KO medaka. Red bars represent up-regulated genes, and blue bars represent down-regulated genes in KO medaka.

Fig. 4 *LDAIR* KO fish show decreased self-protective behaviors in LD conditions.
a Effect of photoperiod on whole body cortisol levels (**P* < 0.05, *t*-test; mean ± SEM, n = 4). Horizontal bars indicate means, and dot plots indicate individual data points. **b** Schematic drawing of the apparatus for the novel tank test. **c** Results of novel tank test under SD (top) and LD (bottom) conditions showing total vertical activity (left) and freezing duration (right) in wild type (WT) and knockout (KO) fish (***P* < 0.01, *t*-test; mean ± SEM, n = 16). Horizontal bars indicate means, and dot plots indicate individual data points. **d** Schematic drawing of the apparatus for the light dark tank test. **e** Results of light dark tank test under SD (top) and LD (bottom) conditions showing total time spent in light area (left) and number of transitions (right) between WT and KO (**P* < 0.05, *t*-test; mean ± SEM, top; n = 16, bottom; n = 20). Horizontal bars indicate means, and dot plots indicate individual data points. Note, to compare sufficient numbers of WT and KO fish, we performed LD and SD experiments on different days, due to experimental limitations. We therefore cannot compare the results of LD and SD directly.

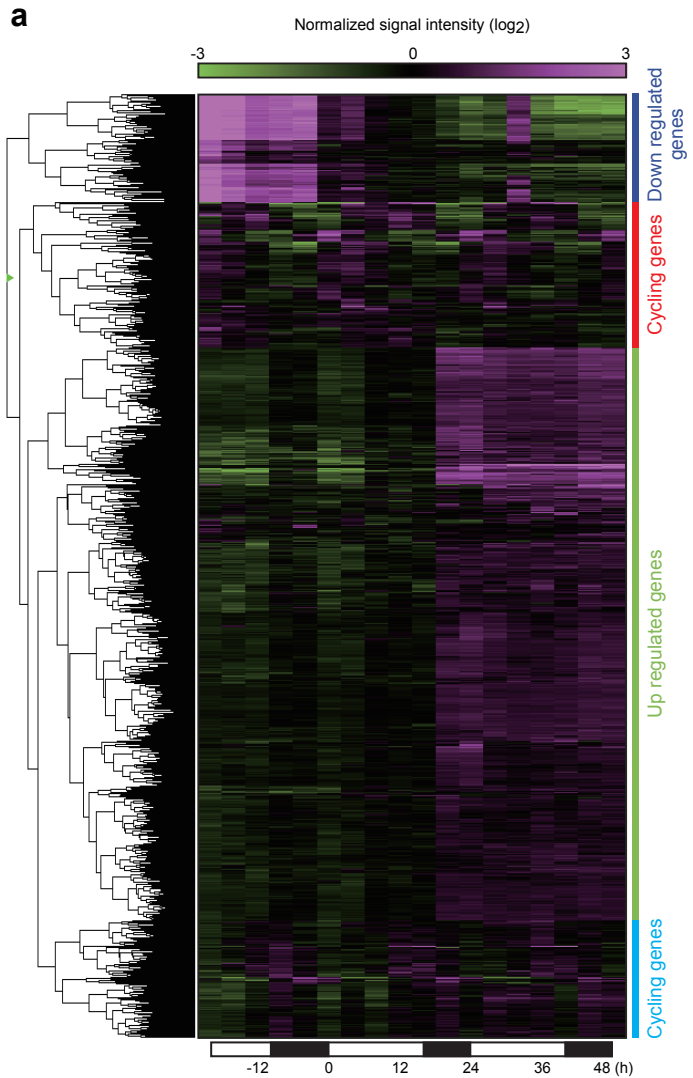

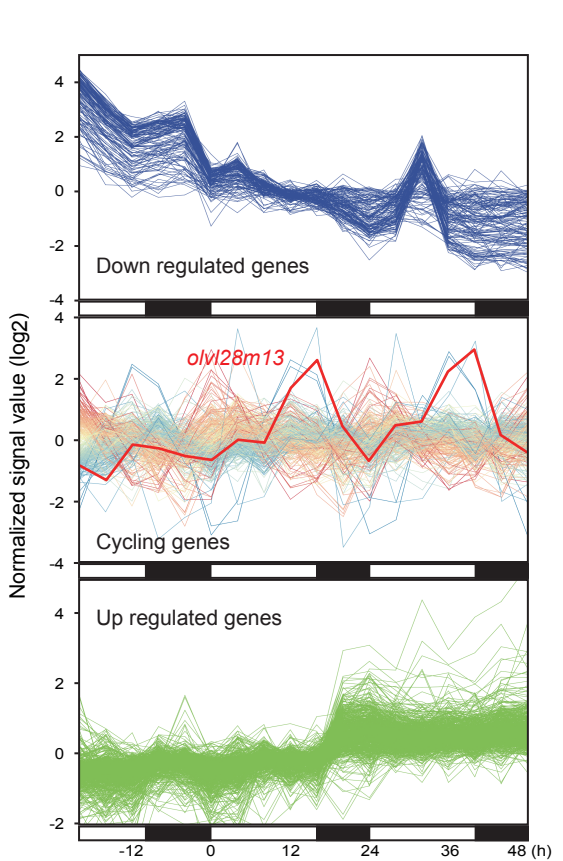

c

Ingenuity Canonical Pathways	P-value
FXR/RXR Activation	5.2E-05
LXR/RXR Activation	4.4E-04
Ubiquinol-10 Biosynthesis	6.6E-04
Acute Phase Response Signaling	9.3E-04
Cholesterol Biosynthesis	9.5E-04

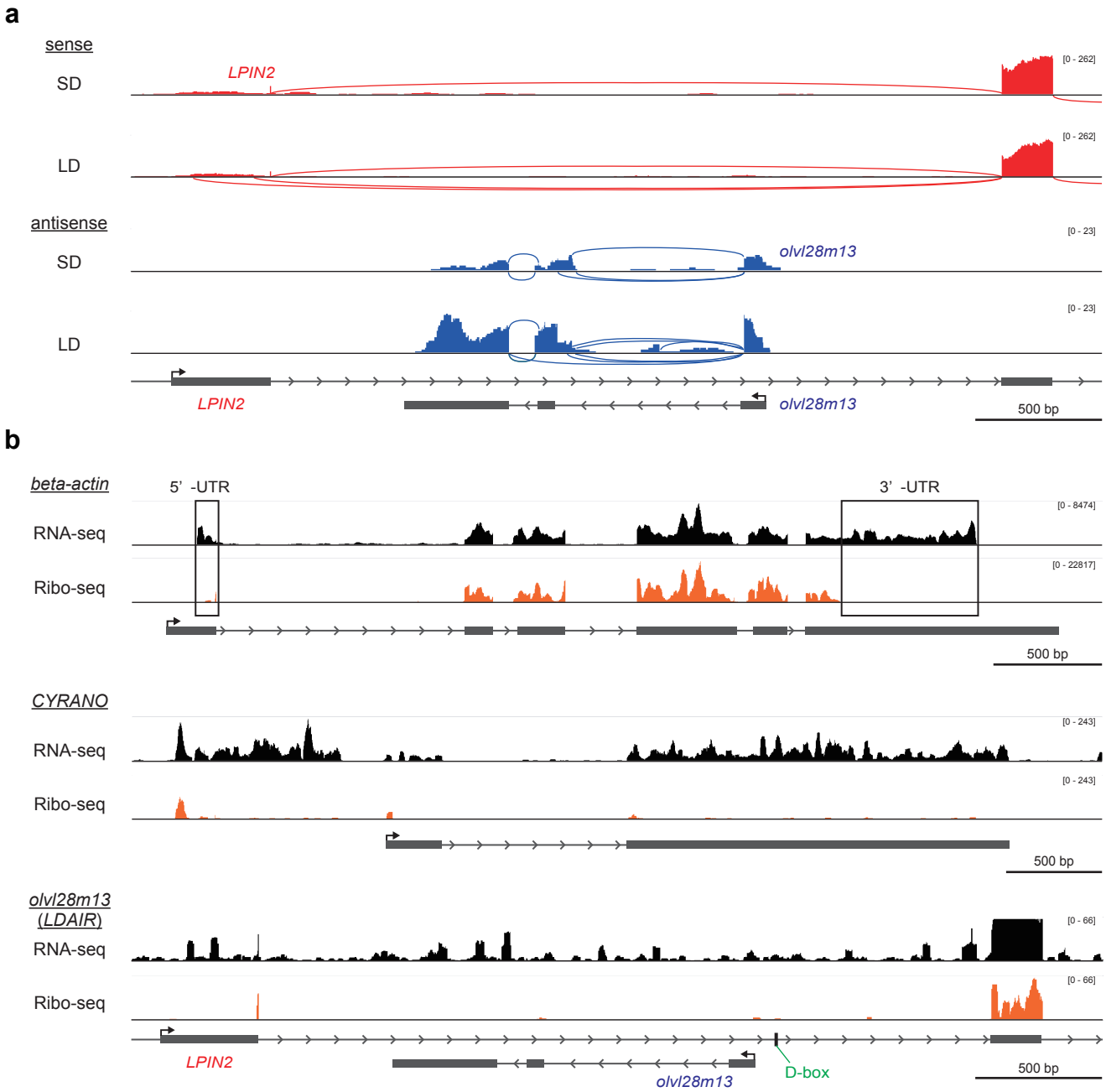
a
sense
SD
LPIN2
[0 - 262]
LD
[0 - 262]
antisense
SD
olvl28m13
[0 - 23]
LD
[0 - 23]
LPIN2
olvl28m13
500 bp
b
beta-actin
5' -UTR
3' -UTR
RNA-seq
[0 - 8474]
Ribo-seq
[0 - 22817]
500 bp
CYRANO
RNA-seq
[0 - 243]
Ribo-seq
[0 - 243]
500 bp
olvl28m13
(LDAIR)
RNA-seq
[0 - 66]
Ribo-seq
[0 - 66]
LPIN2
olvl28m13
D-box
500 bp

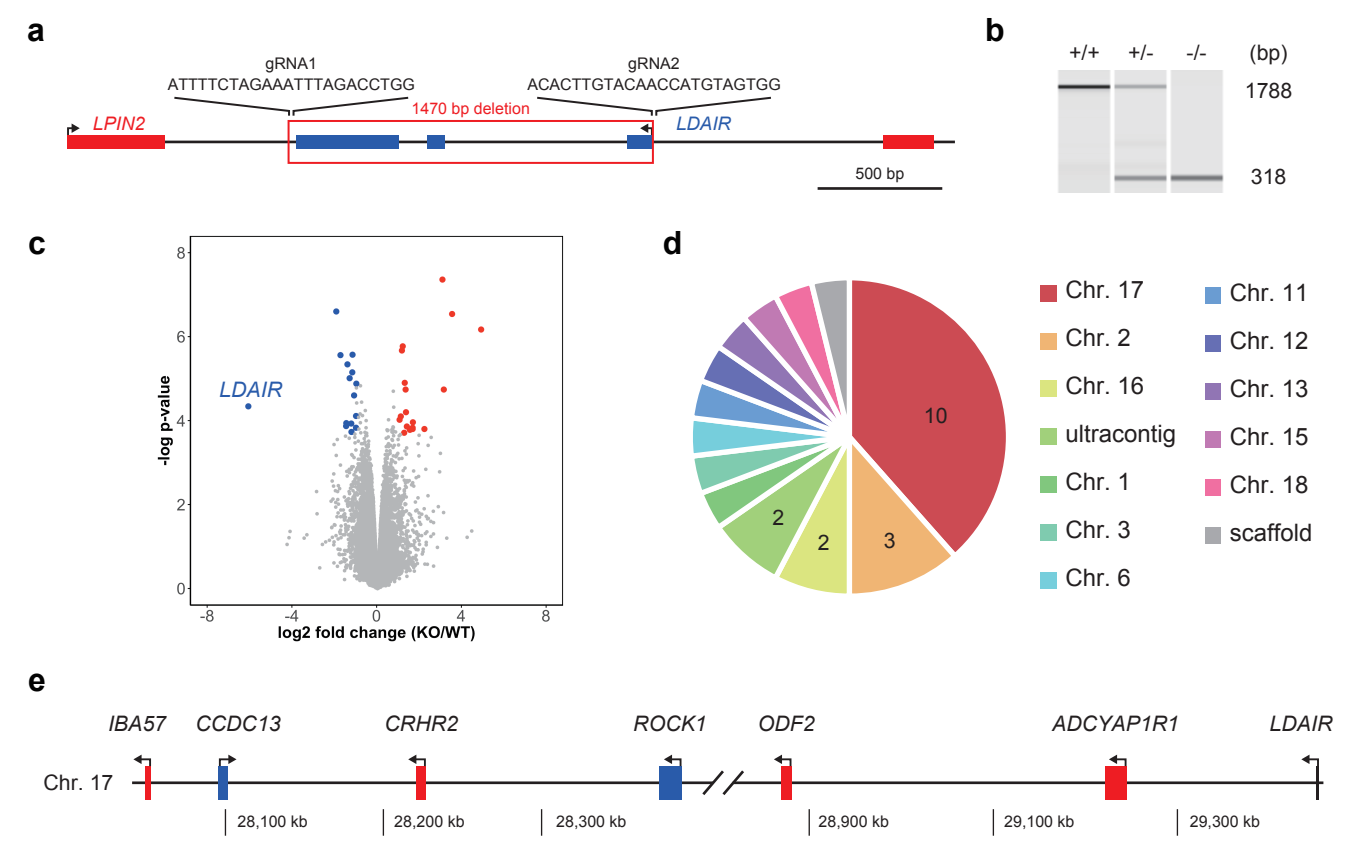
a
gRNA1
ATTTTCTAGAAATTTAGACCTGG
gRNA2
ACACTTGTACAACCATGTAGTGG
1470 bp deletion
LPIN2
LDAIR
500 bp
b
+/+
+/-
-/-
(bp)
1788
318
c
LDAIR
-log p-value
log2 fold change (KO/WT)
d
Chr. 17
Chr. 2
Chr. 16
ultracontig
Chr. 1
Chr. 3
Chr. 6
Chr. 11
Chr. 12
Chr. 13
Chr. 15
Chr. 18
scaffold
10
3
2
2
e
IBA57
CCDC13
CRHR2
ROCK1
ODF2
ADCYAP1R1
LDAIR
Chr. 17
28,100 kb
28,200 kb
28,300 kb
28,900 kb
29,100 kb
29,300 kb

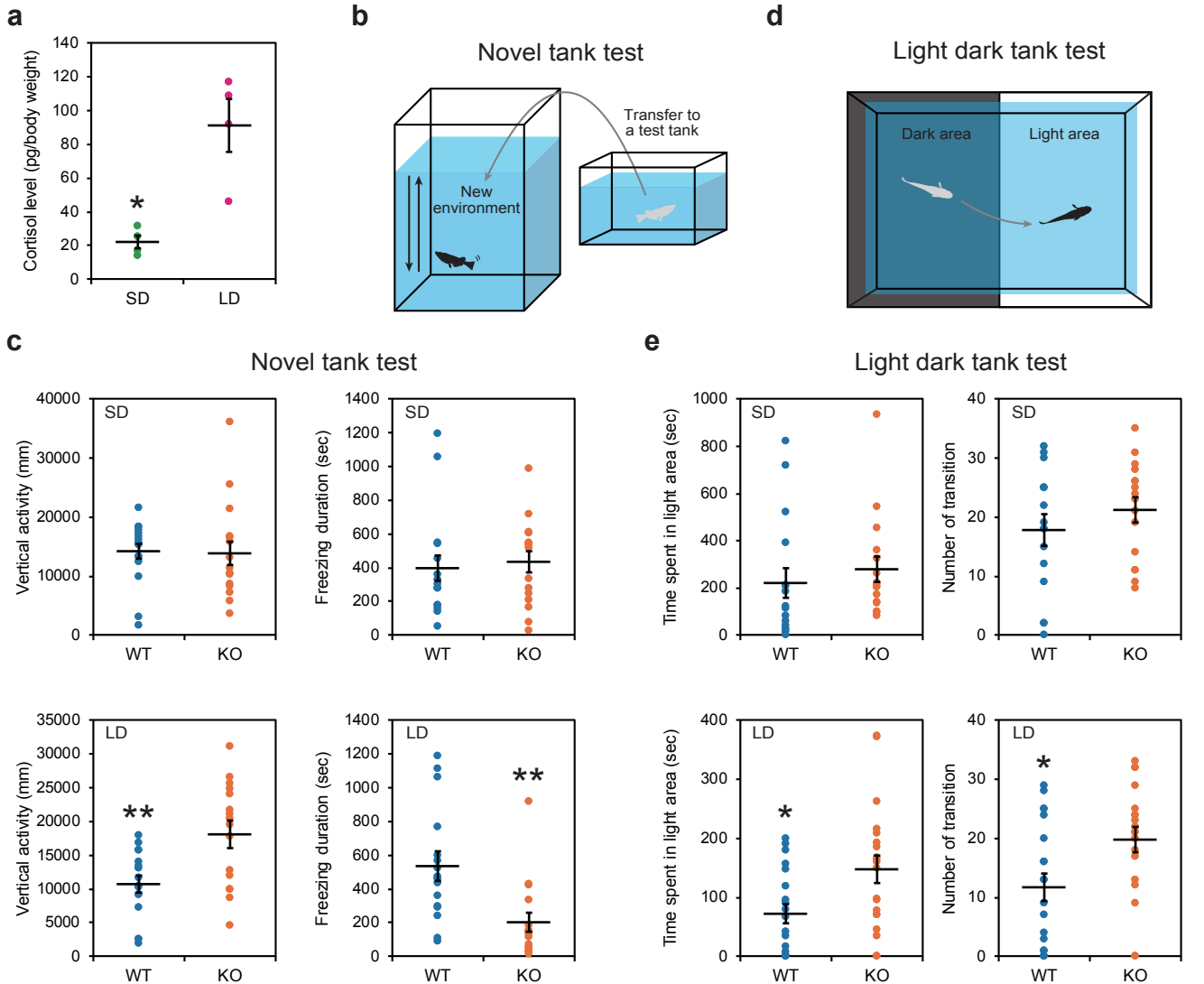
a
Cortisol level (pg/body weight)
140
120
100
80
60
40
20
0
*
SD
LD
b
Novel tank test
Transfer to
a test tank
New
environment
d
Light dark tank test
Dark area
Light area
c
Novel tank test
Vertical activity (mm)
40000
30000
20000
10000
0
SD
WT
KO
Freezing duration (sec)
1400
1200
1000
800
600
400
200
0
SD
WT
KO
35000
30000
25000
20000
15000
10000
5000
0
LD
**
WT
KO
1400
1200
1000
800
600
400
200
0
LD
**
WT
KO
e
Light dark tank test
Time spent in light area (sec)
1000
800
600
400
200
0
SD
WT
KO
Number of transition
40
30
20
10
0
SD
WT
KO
400
300
200
100
0
LD
*
WT
KO
40
30
20
10
0
LD
*
WT
KO